OPTOELECTRONICS AND ADVANCED MATERIALS – RAPID COMMUNICATIONS Vol. 11, No. 11-12, November-December 2017, p. 652-658

Downlink transmission in coherent passive optical network at 400 Gbps using digital signal processing

GAURAV PANDEY*, ADITYA GOEL
Maulana Azad National Institute of Technology, Department of ECE, Bhopal-462003, M.P., India

Here 400 Gbps downlink Coherent Passive Optical Network (CPON) transmission has been demonstrated over 81 km of Standard Single Mode Fiber (SSMF) using Dual Polarization-16-Quadrature Amplitude Modulation at the central office with Digital Signal Processing (DSP) at the Optical Network Unit (ONU) and 1:64 power split at Remote Node. Adaptive DSP is employed at ONU to compensate the linear impairments caused by 400Gbps optical signal transmission over 81 km SSMF. The results obtained by simulation indicate that the proposed 400Gbps downlink transmission of CPON is practicable. The proposed high speed CPON may be exercised for the realization of the Next-Generation PONs.

(Received March 7, 2017; accepted November 28, 2017)

Keywords: Quadrature Amplitude Modulation (QAM), Coherent Passive Optical Network (CPON,) Central Office (CO), Digital Signal Processing (DSP)

1. Introduction

Due to exponential increase in bandwidth demand by broadband communication networks, wavelength division multiplexed – passive optical network (WDM-PON) has become a potential candidate for next generation optical access networks. WDM PONs provides various advantages like channel independency, security, upgradability, high capacity and excessive power budget [1-3]. Recently for broadband optical networks, PONs are widely installed.

It is well known that chromatic dispersion (CD) and polarization mode dispersion (PMD) are severely limiting factor for transmission distance in higher data rate networks like 100 Gbps or 400 Gbps [4]. Hence, for point to multipoint PONs, it is necessary to compensate the fiber dispersion caused by the different length of the fiber from central office (CO) to optical network unit (ONU).

Coherent detection is an eye catching solution for the implementation of large capacity, long reach and high power splitting that is to be used in next-generation (NG)-PONs. Furthermore, coherent PON (CPON) make use of passive technology to increase the power budget. CPON directly applies the optical coherent technology into the NG-PONs. As coherent detection technology is already widely installed in backbone networks, it is expected that it will be employed in high speed PONs in near future. In the coherent detection technology, the dispersion compensation is done in the digital domain using digital signal processing (DSP) and power budget will increase [5, 6]. The sampling rate of analog to digital converter (ADC) can be decreased by decreasing the symbol rate. This can be realized by utilizing dual polarization (DP) technique in coherent technology for the implementation of high speed networks. Previously CPON has been implemented experimentally for transmission over 40 km optical fiber and with a power splitter of 1:1024, however the data rate utilized for the implementation of CPON is very low i.e. 5 Gbps [7]. In literatures, dispersion compensating fiber (DCF) has been employed for dispersion compensation in optical transmission system are likely to increase the complexity and cost of the system [8-9].

In this paper we have demonstrated 400 Gbps downlink transmission in CPON over 81 km transmission distance using Dual Polarization-16-Quadrature Amplitude Modulation (DP-16-QAM) and 1:64 power split. Linear impairments generated by high speed (400 Gbps) optical signal transmission over 81 km standard single mode fiber (SSMF) are mitigated in the digital domain by employing DSP at receiving end (ONU). In view of the fiber nonlinearity, the launched power into optical fiber has been optimized for highest power budget and used for the calculation of corresponding receiver sensitivity for BER of 10^{-9}. The colorless upstream transmission may be added easily in the proposed architecture by utilization of a reflective semiconductor optical amplifier (RSOA) at ONU [10-13]. Additionally WDM technology can be employed to further improve the performance and to achieve more data carrying capability.

2. Proposed architecture

Fig. 1 shows the schematic of the proposed architecture for 400 Gbps coherent detection downlink transmission over 81 km SSMF (80 km feeder fiber + 1 km distribution fiber) and 1:64 split using DP-16-QAM. Fig. 2 (a) shows the schematic of DP-16-QAM transmitter. To generate a DP-16-QAM signal, a continuous wave (CW) laser beam at 1550 nm

wavelength and 100 kHz line width has been used. A polarization splitter with a device angle of 45^0 has been employed to split the CW laser beam into two polarizations. The serial pseudo random binary sequence (PRBS) data (length = $(2^{31}-1)$) has been converted into two parallel data streams by utilizing a serial to parallel converter. The two parallel data streams of PRBS data are modulated on each polarization of CW laser using 16-QAM modulation for each polarization to produce a 400 Gbps DP-16-QAM signal at the CO. Each $LiNbO_3$ Mach-Zehnder modulator (MZM) has an extinction ratio of 30 dB. The output power of DP-16-QAM has been set to 10 dBm.

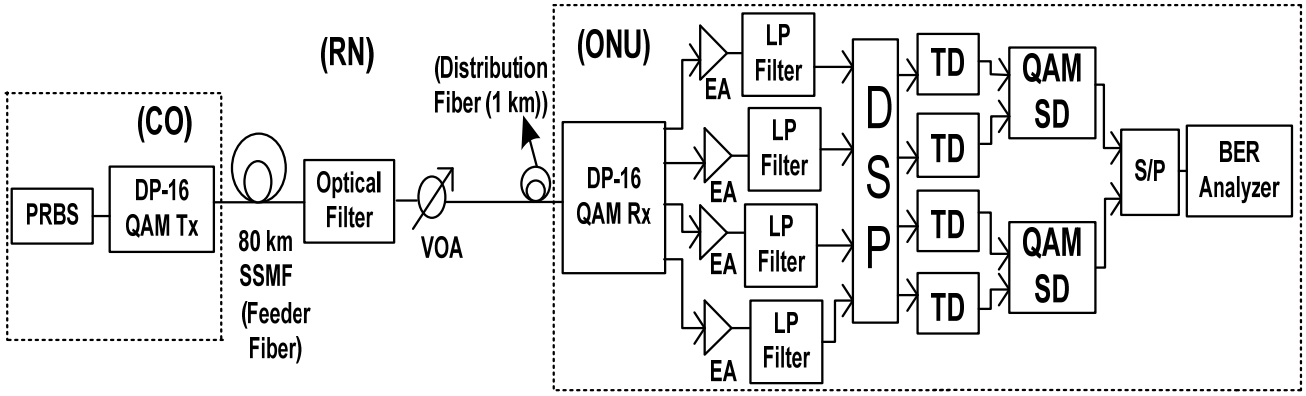

Fig. 1. Schematic of 400 Gbps capable downlink transmission in PON using DP-16QAM and DSP (DP: dual polarization, PRBS: pseudo random binary sequence, VOA: variable optical attenuator, LP: low pass, TD: threshold detector, SD: sequence detector, BER: bit error rate, DSP: digital signal processing, S/P: serial to parallel converter)

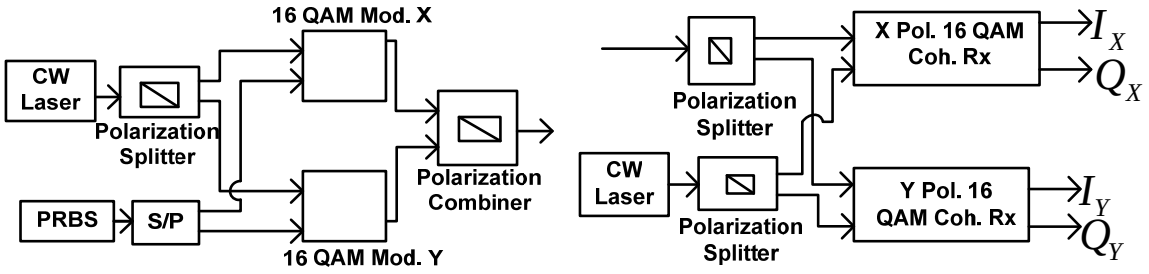

(a) (b)

Fig. 2. Schematic of (a) 400 Gbps DP-16 QAM transmitter (b) DP-16 QAM receiver

The output DP-16-QAM signal from the CO has been fed to 80 km feeder SSMF. The different parameter of SSMF has been set as: dispersion = 16.75 ps/nm.km, dispersion slope = 0.075 ps/nm^2.km and attenuation = 0.2 dB/km. The output of SSMF has been given to an optical filter. The unwanted signals have been filtered out by an optical filter with central wavelength equal to 1550 nm and bandwidth equal to 1 nm. The output of filter has been given to variable optical attenuator (VOA). VOA works analogous to 1:64 power splitter with an attenuation loss equal to 20.5 dB (power splitter loss = 18 dB + excess loss = 2.5 dB). VOA output has been given to the DP-16-QAM receiver after passing through 1 km distribution fiber results in 4 output signals, i.e. In-phase (I) and Quadrature phase (Q) components of X and Y polarizations of 16-QAM signal. Fig. 2(b) shows the schematic of the DP-16-QAM receiver where a local oscillator and a polarization splitter (device angle = 45^0) is utilized for the coherent detection of each polarization of 16-QAM signal. PIN photodetector has been used in the simulation with dark current equals to 10 nA and responsitivity equal to 1A/W. After that the I and Q output of each polarization from DP-16-QAM receiver have been given to DSP for digital domain processing. Each coherently detected I and Q-component of 2 polarizations is electrically amplified by using an electrical amplifier (gain = 15 dB and noise power = -100 dBm), low pass filtered by use of a Gaussian low pass filter (cutoff frequency = bitrate/4, insertion loss = 0 dB, depth = 100 dBm and order = 2) and given to DSP component for digital domain processing to compensate the losses caused by the fiber transmission.

Fig. 3 shows the basic schematic for the construction of the DSP. After coherent detection of the DP-16-QAM signal, the DSP will compensate for the linear impairments of the optical fiber for DP 16-QAM modulation format in the digital domain through the

following functions: conversion of analog signal to digital signal through ADC, compensation of chromatic dispersion (CD), polarization de-multiplexing, estimation of carrier phase and in last conversion of digital signal back to an analog signal through DAC. The algorithms used for the implementation of DSP are realized by utilizing MATLAB software.

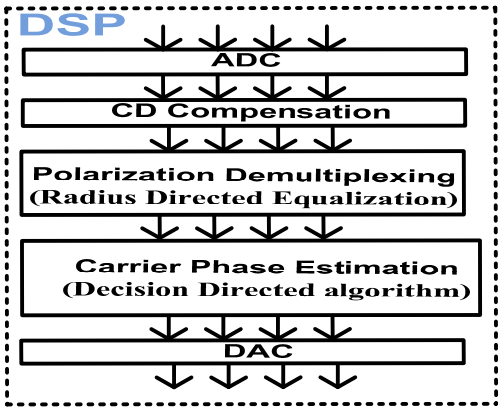

Fig. 3. Schematic for the construction of DSP

Basically, the analog to digital conversion is a down sampling process and is implemented using the ADC with parameters as: symbol rate = (bitrate)/8, number of symbols = (sequence length)/8 and samples per symbol = 4. Dispersion compensation has been implemented by using an easy transversal digital filter. In the absence of nonlinearity of an optical fiber, it can be represented as a phase only filter by using the below transfer function [14]:

$$G(z,\omega) = \exp\left(-j\frac{D\lambda^2 z}{4\pi c}\omega^2 + j\frac{S\lambda^4\omega^3 z}{24\pi^2 c^2}\right) \qquad (1)$$

Here the first component characterizes the dispersion of an optical fiber and the second component characterizes the dispersion slope for applications such as multi-channel operations. Dispersion compensation has been achieved by multiplying the output field to the inverse of the channel transfer function. As the amount of dispersion (length of the propagation) increases, the order of the filter should also increase [14] for more dispersion compensation. In the implementation of dispersion compensation through simulation, the parameters are set as: channel wavelength = 1550 nm, dispersion reference wavelength = 1550 nm, fiber residual dispersion = 16.75 ps/nm-km, tap number = 199 and residual dispersion slope = 0.075 ps/nm^2-km.

Polarization multiplexing is done by radius directed equalization (RDE) algorithm. For QAM signals, an alternative error criterion is the error between the received signal and the nearest constellation radius [15] and termed as RDE. This method adapts the Constant-Modulus Algorithm (CMA) to the 16-QAM constellation. Fig. 4 shows the non-constant modulus of 16-QAM.

We remind that the received signal has been sampled at the twice the baud rate in order to satisfy Shannon-Nyquist sampling theorem. Therefore, in order to compensate for the channel impulse response, we have to introduce a Ts/2-Fractionally Spaced Equalizer (FSE). Let $z_p(n)$ be the scalar output of the FSE associated with the polarization p. The cost function in RDE equalization [16, 17] is:

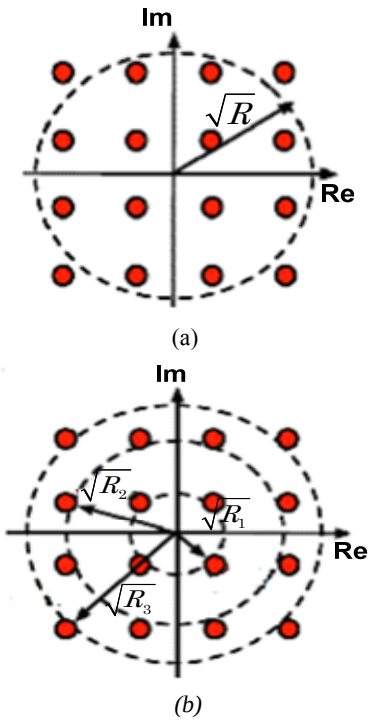

Fig. 4. Non-constant modulus of 16-QAM used for (a) CMA (b) RDE equalization [15]

$$J_{RDE}(w_p) = E\left[J_{RDE,n}(w_p)\right] \qquad (2)$$

With

$$J_{RDE,n}(w_p) = \left(|z_p(n)|^2 - R_0\right)^2 \qquad (3)$$

Where $E[\cdot]$ indicates statistical expectation and $z_p(n)$ is the equalizer output. R_0 is the constant depending only on the input data symbol. Where R_0 is given by:

If $|z_p(n)| < \left(\sqrt{R_1} + \sqrt{R_2}\right)/2$ then point belongs to group 1 and $R_0 = R_1$

else

If $|z_p(n)| < \left(\sqrt{R_2} + \sqrt{R_3}\right)/2$ then point belongs to group 3 and $R_0 = R_3$

else

point belongs to group 2 and $R_0 = R_2$

end if

end if

In 16-QAM modulation, $R_1 = 0.2$, $R_2 = 1$, and $R_3 = 1.8$. The rest of the algorithm is the same as CMA used in the DSP for DP-QPSK [18]-

Initial value 1:

$p_{xx}(0) = [00\ldots010..00];$
$p_{yy}(0) = [00\ldots010..00];$
$p_{xy}(0)=p_{yx}(0)= [00\ldots000..00];$

Initial value 2:

$p_{xy}(0) = [00\ldots010..00];$
$p_{yx}(0) = [00\ldots010..00];$
$p_{xx}(0)=p_{yy}(0)= [00\ldots000..00];$

Initial value 3:

$p_{xx}(0) = [00\ldots010..00];$
$p_{yx}(0) = [00\ldots010..00];$
$p_{xy}(0)=p_{yy}(0)= [00\ldots000..00];$

Initial value 4:

$p_{xy}(0) = [00\ldots010..00];$
$p_{yy}(0) = [00\ldots010..00];$
$p_{yx}(0)=p_{xx}(0)= [00\ldots000..00];$

To compensate the phase and frequency disparity between the transmitters and LO, a carrier phase estimator using decision directed carrier phase recovery algorithm [19] is utilized. This algorithm works on each polarization simultaneously. Fig. 5 demonstrated the block diagram of the decision directed carrier phase algorithm.

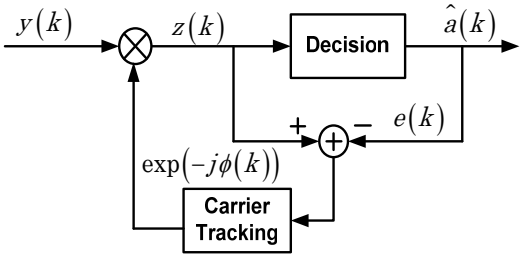

Fig. 5. Schematic for Decision directed carrier phase algorithm [19]

In the decision directed (DD) algorithm, the error is calculated between the output of the equalizer from the previous stage and the corresponding decision. The phase is updated by the following equation [19, 20]:

$$\hat{\phi}(k+1) = \hat{\phi}(k) - \mu_{\phi}\Im_m\left[z(k)e^{*}(k)\right] \quad (4)$$

$$J_{RDE,n}(w_p) = \left(\left|z_p(n)\right|^2 - R_0\right)^2 \quad (5)$$

Where μ_{φ} is the step size and the error function $e(k)$ is given by:

$$e(k) = z(k) - \hat{a}(k) \quad (6)$$

$$z(k) = y(k)\exp\left(-j\phi(k)\right) \quad (7)$$

Where z(k) is the equalized output with phase error correction and a(k) is the estimation of z(k) by a decision device. To compute the constellation diagrams we ignored 100 symbols from starting and the end. The interpolation method used for DAC is step.

3. Results and discussion

Here the architecture as shown in Fig. 1 has been simulated. Table 1 shows the specification of different parameters that are utilized for simulation. The optical spectrum of the 400 Gbps DP-16-QAM signal after the transmitter and the RF spectrum after the coherent DP-16-QAM receiver have been shown in Fig. 6(a) and Fig. 6(b) respectively, for X-polarization I component.

Table 1. Specification of different simulation parameters

S. No.	Parameter	Specification
1.	Fiber Length	Feeder fiber = 80 km Distribution fiber = 1 km
2.	Bits per symbol	4
3.	Transmitting Wavelength	1550 nm
4.	Symbol Rate for DSP	Bit rate/8
5.	Number of Samples for DSP	Sequence length/8
6.	Transmit power	10 dBm
7.	Bit Rate	400 Gbps
8.	Sequence Length	65536 bits
9.	Samples per bit	8
10.	Number of samples	524288
11.	Interpolation	step

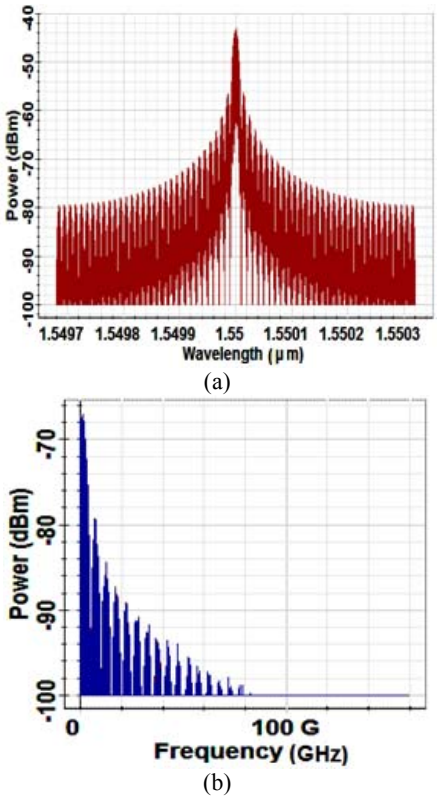

Fig. 6. Spectrums for I component of X-polarization (a) 400 Gbps DP-16-QAM signal's Optical spectrum at the transmitter (b) RF spectrum acquired at the coherent DP-16-QAM receiver

Fig. 7(a) shows the RF spectrum obtained after the coherent low pass Gaussian filter and Fig. 7(b) shows the RF spectrum obtained after the DSP for I component of X-polarization.

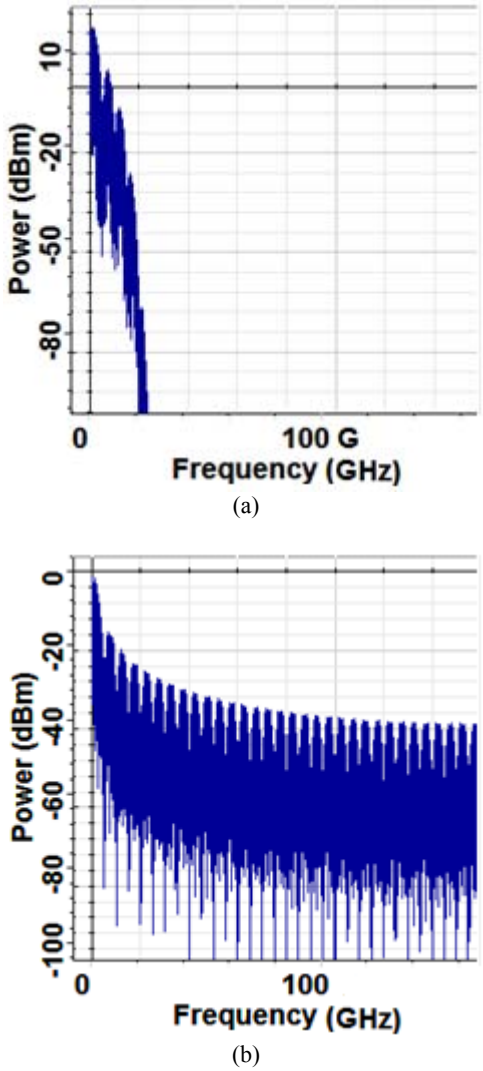

Fig. 7. RF spectrum obtained for I-component of X-polarization DP-16QAM signal (a) after the coherent low pass Gaussian filter (b) after the DSP

Fig. 8(a) shows the constellation diagram of downlink X-polarized 16-QAM signal before DSP and Fig. 8(b) shows the constellation diagram of downlink X-polarized 16-QAM signal after DSP. Here red and blue colours represent signal and noise respectively. It is evident from figures that only by the implementation of DSP; the data has been retrieved correctly.

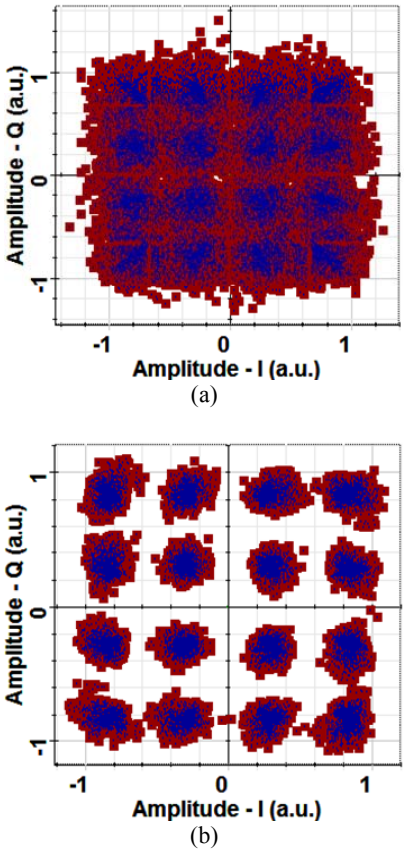

Fig. 8. X-polarization signal constellation diagram (a) before DSP (b) after DSP

The curve of measured bit error rate (BER) versus received optical power for the DP-16-QAM 400 Gbps coherent transmission over 81 km optical fiber and back to back (B2B) has been shown in Fig. 9(a). The received optical power is -28.24 dBm and -28 dBm for B2B and 80 km transmission respectively for BER = 10^{-9}. Dispersion compensation causes a receiver sensitivity penalty equal to 0.24 dB only. Dispersion compensation greater than 1357 ps/nm (corresponding to 81 km SSMF) has been provided by the DSP adaptive equalization.

The curve of launching power into optical fiber versus receiver sensitivity has been shown in Fig. 9(b) for transmission over 81 km. The nonlinear effects increase in an optical fiber with the increase of the launched optical power into the optical fiber span. Here received optical power has been calculated at different launched optical power into the fiber span. In this for 10 dBm input optical power, best receiver sensitivity of -28 dBm has been achieved at BER = 10^{-9}. Further, best power budget of 38 dB has been achieved for launching power of 10 dBm.

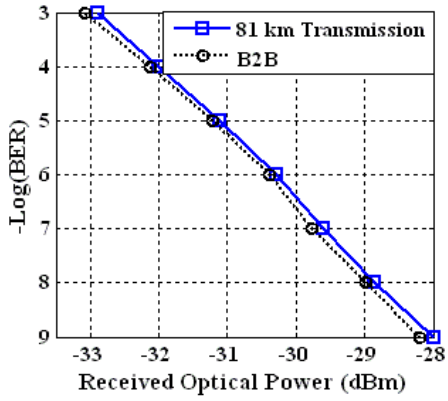

(a)

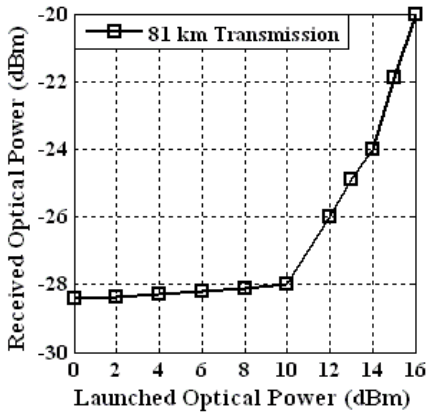

(b)

Fig. 9. Curve of (a) BER versus received optical power over 81 km and B2B transmission (b) Receiver sensitivity versus launched optical power into an optical fiber link for transmission over 81 km SSMF

Fig. 10 shows plot of BER versus the optical to signal ratio (OSNR) for back to back (B2B) and 81 km transmission of the proposed architecture along with the expected theoretical values for 400 Gbps DP-16-QAM transmission. For a BER of 10^{-9}, 46 dB OSNR is required. The maximum power penalty between B2B transmission and 81 km transmission is of the order of 0.4 dB, tells that chromatic dispersion caused by optical fiber transmission is negligible.

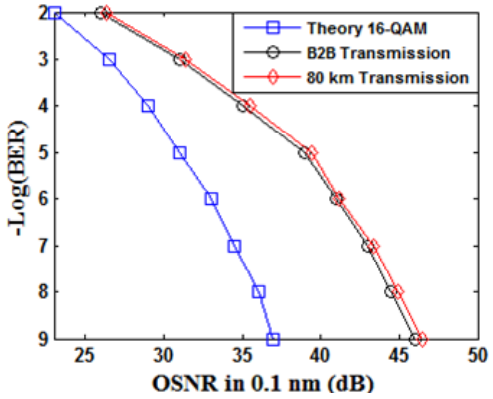

Fig. 10. OSNR sensitivity for 400 Gbps DP-16-QAM transmission

The results for X and Y polarizations at different stages of DSP have been shown in Fig. 11. Fig. 11(a) and 11(b) show constellation diagram of received signal after CD dispersion for X and Y-polarizations respectively using DSP. Fig. 11(c) and 11(d) show constellation diagram of received signal after polarization demultiplexing for X and Y-polarizations respectively using DSP. Fig. 11(e) and 11(f) show constellation diagram of received signal after carrier phase estimation for X and Y-polarizations respectively using DSP.

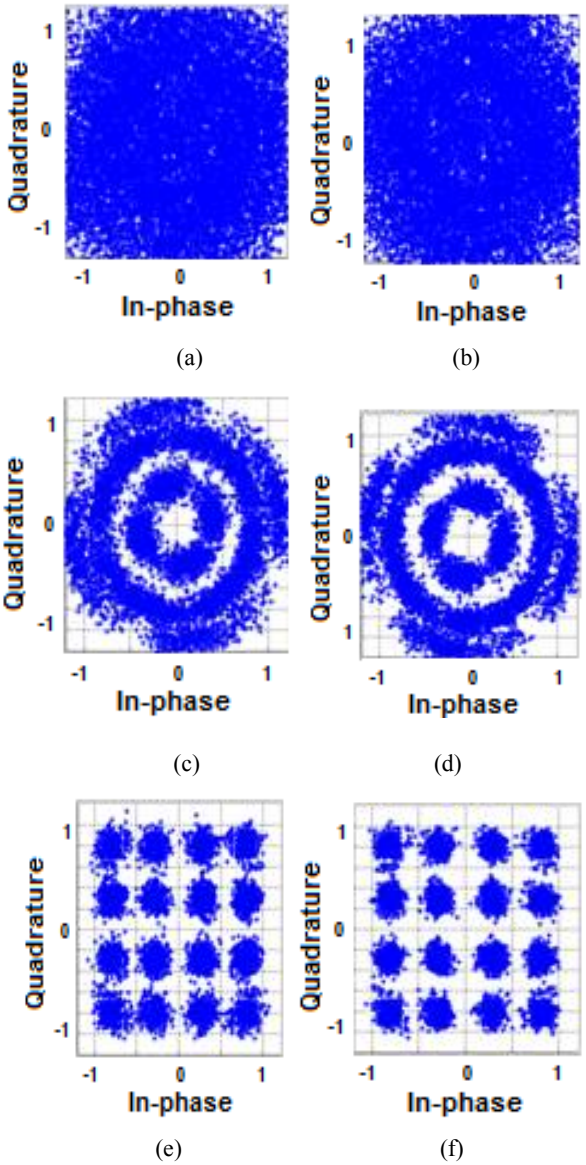

(a) (b)

(c) (d)

(e) (f)

Fig. 11. Received signal constellation diagram using DSP (a) after CD dispersion for X-Polarization (b) after CD dispersion for Y-Polarization (c) after polarization demultiplexing for X-Polarization (d) after polarization demultiplexing for Y-Polarization (e) after carrier phase estimation for X-Polarization (f) after polarization demultiplexing for Y-Polarization

Fig. 12 shows the number of users (split at RN) supported at 400 Gbps for downstream signal transmission over different distance when BER = 10^{-9}. At 400 Gbps, 64 number of users can be supported till 81 km. As the number of split increase, supported transmission distance starts decreasing due to increased loss of optical power splitter present at RN. For 1024 number of users, the transmission distance of 21 km can be supported. As the number of split decrease, supported transmission distance starts increasing due to decreased loss of optical power splitter present at RN. For 32 number of users, the transmission distance of 96 km can be supported.

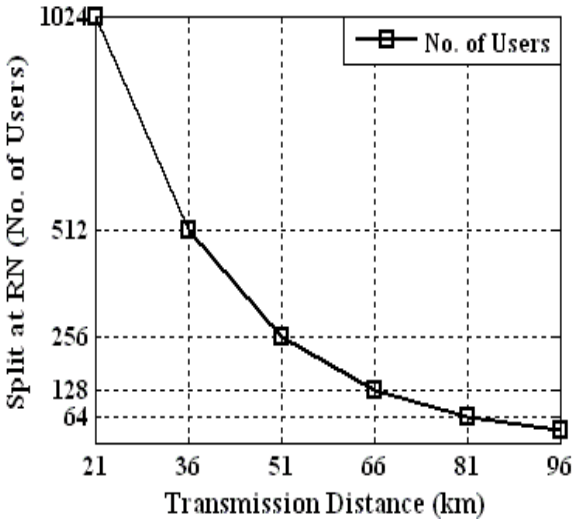

Fig. 12. Plot for split at RN (No. of users) at different transmission distance (BER = 10^{-9})

4. Conclusion

Here downlink transmission of 400 Gbps CPON has been analyzed over 81 km SSMF using DP-16-QAM with digital signal processing (DSP) and 1:64 power split. In fiber non-linearity conditions, received optical power of -28 dBm has been achieved for BER = 10^{-9}. Receiver sensitivity decreases with the increase in launched optical power. By accounting the fiber non-linearity, the optimal launched power for highest power budget is found to be 10 dBm and the corresponding receiver sensitivity is -28 dBm for BER = 10^{-9} over 81 km SSMF transmission. Here maximum power budget of 38 dB has been achieved for the launched power of 10 dBm. In the implementation of high speed, extended reach and enhanced capacity NGPONs, the proposed downlink transmission of 400 Gbps DP-16-QAM CPON over 81 km optical fiber with 1:64 power split may be demonstrated as a feasible solution. Also, 400 Gbps coherent PON is a strong nominee technology for next generation high speed PONs.

References

[1] T. Koonen, ECOC, Brussels, paper We.2.A.1, 1 (2008).
[2] N. Cvijetic, D. Qian, J. Hu, IEEE Commun. Mag. **48**(7), 70 (2010).
[3] P. P. Iannone, K. C. Reichmann, ECOC, Torino, paper Tu.B.3.1 (2010).
[4] D. Qian, S-H. Fan, N. Cvijetic, J. Hu, T. Wang, OFC/NFOEC, Los Angeles, paper OMG4 (2011).
[5] S. J. Savory, Proc. SPIE **7136**, Optical Transmission, Switching, and Subsystems VI, 71362C (2008).
[6] G. Lachs, S. M. Zaidi, A. K. Singh, J. Lightw. Tech. **12**(6), 1036 (1994).
[7] J. B. Jensen, R. Rodes, D. Zibar, I. T. Monroy, OFC/NFOEC, Los Angeles, paper OTuB2 (2011).
[8] A. Goel, G. Pandey, IEEE Journal of Selected Topics in Quantum Electronics **22**(2), 100 (2016).
[9] G. Pandey, A. Goel, Optical and Quantum Electronics **46**(12), 1509 (2014).
[10] S. Mhatli, M. Ghanbarisabagh, L. Tawade, B. Nsiri, M. A. Jarajreh, M. Channoufi, R. Attia, Optics Letters **39**(23), 6668 (2014).
[11] G. Pandey, A. Goel, Optik **124**(23), 6245 (2013).
[12] G. Pandey, A. Goel, Optik **125**(17), 4951 (2014).
[13] G. Pandey, A. Goel, Optical Engineering (SPIE), **55**(7), 076101-1 (2016).
[14] S. J. Savory, Opt. Express **16**(2), 804 (2008).
[15] M. Selmi, PhD thesis, Doctoral School of Computer Science, Telecommunications and Electronics of Paris (2011).
[16] S. J. Savory, IEEE Journal of Selected Topics in Quantum Electronics, **16**(5), 1164 (2010).
[17] M. Ready, R. Gooch, International Conference on Acoustics, Speech, and Signal Processing, 1990 (ICASSP-90), **3**, 1699 (1990).
[18] G. Pandey, A. Goel, Optical and Quantum Electronics, Springer **47**(11), 3445 (2015).
[19] I. Fatadin, D. Ives, S. J. Savory, Journal of Lightwave Technology **27**(15), 3042 (2009).
[20] G. Picchi, G. Prati, IEEE Trans. Commun. **35**(9), 877 (1987).

*Corresponding author: gauravpandeymanit@gmail.com